NASA scatterometer provides global ocean-surface wind fields with more structures than numerical weather prediction

W. Timothy Liu, Wenqing Tang, and Paulo S. Polito

Jet Propulsion Laboratory, California Institute of Technology, Pasadena, CA

Abstract. The major differences between monthly-mean ocean-surface wind fields derived from the observations of the National Aeronautics and Space Administration (NASA) Scatterometer (NSCAT) and produced by the operational numerical weather prediction (NWP) model of the European Center for Medium-Range Weather Forecasts are found in coastal and equatorial regions, where the sharp changes are smoothed over in NWP products; these wind differences are explained to be the result of the superior spatial resolution of NSCAT winds. Objective interpolation of NSCAT data alleviates errors caused by the uneven satellite sampling and retains superior energy content of NSCAT winds at high wavenumbers.

1. Introduction

The National Aeronautics and Space Administration (NASA) Scatterometer (NSCAT) was successfully launched into a near-polar and sun-synchronous orbit on the Japanese Advanced Earth Observation Satellite (ADEOS-1) in August 1996. About nine months of data, from 15 September 1996 to 29 June 1997, were collected before the failure of ADEOS. From NSCAT observations, surface wind vectors (speed and direction) at 10-m height were derived at 25-km spatial resolution, covering approximately 77% of the Earth's oceans in one day and 87% in two days, under both clear and cloudy conditions. Validation studies consisting of point-to-point comparisons with in situ measurements [e.g., Bourassa et al., 1997] have shown encouraging results.

Most atmospheric and oceanic studies require uniformly gridded wind fields [e.g., Liu et al. 1997]; products from numerical weather prediction (NWP) have been most frequently used in the recent years. This is a brief report on the global wind fields derived from NSCAT and the comparison with winds produced by the operational NWP model of the European Center for Medium-Range Weather Forecasts (ECMWF). The ECMWF 6-hourly, 1° latitude by 1° longitude, wind fields at the 10-m level are used in this study. This high resolution data set was provided specifically for NSCAT validation.

2. Objective interpolation

A spaceborne sensor, with limited swath width and in polar orbit, can produce only irregular spatial and temporal coverage. Spacebased wind measurements either have to be subjected to averaging within a certain temporal and spatial bin, or be interpolated

with some type of objective method to provide uniformly gridded wind fields. The NSCAT interpolated wind field used in this study has a 0.5° latitude by 0.5° longitude and 12-hourly resolution.

The NSCAT observations were objectively interpolated by the method of successive corrections, proposed by Bergthorsson and Döös [1955] and modified by Cressman [1959]. The interpolation scheme starts with the NSCAT monthly bin-averaged field as an initial guess field. Then, scatterometer observations within the radius of influence (R) and period of influence (T) of the chosen grid point are used to make corrections iteratively. The value of T was chosen to be 1.5 days, and R decreases from 10 grid-spacing to 1 during the 5 successive iterations. The contributions of observations to the correction term were weighted differently according to their positions relative to the grid point under analysis (see Tang and Liu [1996] for more details). Observations were screened out if the difference between them and the interpolated value of the analyzed field exceeded the maximum allowable error (E). E decreases from 50 m/s to 3 m/s over the 5 iterations, allowing increasing confidence in the analyzed field with each successive iteration. The procedure was applied to zonal and meridional wind components separately. Every 12 hours, at 0Z and 12Z, a synoptic field is produced on a grid of 0.5° latitude by 0.5° longitude resolution; the wind field covers all ocean areas from 75°S to 75°N.

The values of T and R were selected as compromises between the desired smoothness of the wind field and the energy it contains. Increasing the two parameters will result in smoother fields but will reduce the energy and decreasing them will give coarser fields and increase the energy. This relatively simple method of successive correction was adopted initially to facilitate fast and continuous production of an interpolated wind field because it is not as computationally demanding and does not require a prior knowledge of atmospheric circulation as other proposed methods [e.g., Legler et al., 1989; Kelly and Caruso, 1990]. Examination of samples of wind fields produced by other methods indicated that these methods do not add much to the findings of this study.

Simple bin-averaging has been used to produce uniformly gridded wind fields in many application of scatterometer data. Zeng and Levy [1995] demonstrated that the patterns of satellite groundtracks are present in satellite wind fields even in monthly bin-averages. Objective interpolation is intended to alleviate this drawback. The approximately north-south-oriented pattern in Fig. 1 represents the ground-track aliasing that is present in the bin-averaged wind field and is removed by the objective interpolation.

3. Wind field comparison

Both the NSCAT and ECMWF wind fields show similar large-scale atmospheric circulation [Liu and Tang, 1997]. They reveal the Hadley circulation with wind converging at the Intertropical Convergence Zone (ITCZ), wind diverging at the Horse Latitudes, and the Trade Winds in-between. They also show the mid-latitude Westerlies with similar cyclones and anticyclones. No significant mean differences have been found between global co-located NSCAT and ECMWF data [M. Freilich, F. Wentz, and N. Ebuchi, personal communication, 1997]. There are, however, large localized differences in the zonal component, as revealed in Fig. 2. The differences in meridional components are smaller and not shown.

Positive (westerly) differences in zonal components in excess of 4 m/s are found off the west coasts of South America and Africa and Australia in Fig.2. These are areas where the Southeast Trades have strong meridional components from the south. The vector comparison off South American in Fig. 3 is used an example for illustration. NSCAT observes much stronger continental influence than is shown in ECMWF winds; NSCAT winds are steered more toward land and, therefore, have a stronger eastward component. The position of the difference shifted with the annual meridional march of the Southeast Trades. In June, there is no significant difference off the west coast of Australia because the influence of the Southeast Trades moves north and the west coast is under the influence of the Westerlies. The NSCAT winds, with their stronger on-shore component, may imply rather different Ekman transport and coastal upwelling than ECMWF winds in these nutrient-rich coastal waters.

There are also large differences in the equatorial oceans. In the example shown in Fig. 4, NSCAT observes a clearer turning of the winds from southeasterly to southwesterly as they cross the equator from the Southern Hemisphere to the Northern Hemisphere. Such turning is less evident in ECMWF winds which remain blowing largely from a southeasterly direction until they meet the Northeast Trades (at the ITCZ north of the equator). Fig. 4 shows that the major eastward vector difference is found just north of the equator. An area of westward difference is also found at 7°N caused by the differences in position and extend of the ITCZ.

The positive differences in zonal components shown in Fig. 2 are mainly caused by differences in wind direction and not wind speed. These areas of differences show up clearly in maps of differences in wind direction (not shown) with the largest angle between NSCAT and ECMWF winds roughly between 45° to 90°. Larger directional difference (up to 180°) are largely found at zonal belts at 40°N and 40°S, at the interface between the Trades and the Westerlies. These two belts can be discerned in Fig. 2 as negative (westward) difference in zonal winds.

4. Wavenumber spectra

Two-dimensional wave spectra in the Northern Pacific (not shown) indicate that NSCAT and ECMWF wind fields have similar levels of energy for wavelengths longer 1000 km. The power decreases rapidly for wavelengths shorter than 300 km. NSCAT winds, however, retain much more power than ECMWF winds at these short wavelengths. Significant loss of small-scale signals is detected in the ECMWF winds as illustrated by the difference in the two-dimensional wavenumber spectra of the zonal components shown in Fig. 3.

5. Conclusion

The characteristics of the differences between NSCAT and ECMWF winds are consistent with the notion that the differences are caused by the higher spatial resolution of (and, therefore, the more realistic representation by) the NSCAT winds, although no objective validation standard is presented. The ECMWF winds in these

areas are characterized by smooth large-scale flow and they miss the sharp gradient caused by land mass and change of Coriolis force at the equator, as detected by the NSCAT winds. This implication is also supported by comparison of the wavenumber spectra, which show that the NSCAT winds include small-scale signals missed by the ECMWF winds. The deficiencies in boundary layer parameterization in the NWP model may be additional cause for the discrepancies. The differences found in this study could have a significant influence on the response of numerical ocean general circulation models forced by the two wind products.

There is no apparent reason to suspect errors in NSCAT winds in the coastal regions. All the NSCAT backscatter observations that include land area have been discarded, and the differences between ECMWF and NSCAT winds can be detected almost 1000 km off shore (NSCAT has 25 km resolution), so the large differences in zonal components, shown in Fig. 2, are not likely to be caused by land contamination of NSCAT data.

In addition to demonstrating the superior utility of NSCAT winds over the present NWP winds, this study also demonstrates that the adverse effects of uneven satellite sampling can be reduced while sufficient energy is retained in the wind field by choosing an optimal interpolation scheme. The satellite data, the interpolation scheme, and the NWP products are undergoing continuous improvement; further evaluation is expected in the future. An improve scatterometer, Quikscat, with similar spatial resolution as NSCAT, but with better coverage is scheduled be launched in November 1998. It will be followed by SeaWinds (the same design), to be launched on ADEOS-2 in the year 2000. The continuous monitoring of ocean-surface winds into the next decade is thus assured.

Acknowledgments. This study was performed at the Jet Propulsion Laboratory (JPL), California Institute of Technology, under contract with the National Aeronautics and Space Administration (NASA). It was supported, in part, by the NASA Scatterometer Project at JPL and NOAA/NASA Enhanced Data Set Studies. It was also jointly supported by NASA's Earth Observation System Interdisciplinary Sciences and Physical Oceanography Programs. We are grateful to the European Center for Medium-Range Weather Forecasts for providing their surface-wind data for NSCAT validation. We are indebted to Gary Lagerloef and Kristina Katsaros for suggestions and comments.

References

Bergthorsson, P., and B. R. Döös, Numerical weather map analysis, Tellus 7, 329-340, 1955.

Bourassa, M.A., M.H. Freilich, D.M. Legler, W.T. Liu, and J. J. O'Brien, Wind observations from new satellite and research vessels agree, *Eos Trans. of Amer. Geophys. Union, 78*, 597 & 602, 1997

Cressman, G. P., An operational objective analysis system, *Mon. Wea. Rev., 87*, 367-374, 1959.

Kelly, K.A., and M.J. Caruso, A modified objective mapping for scatterometer wind data, *J. Geophys. Res., 95*, 13483-13496, 1990.

Legler, D.M., I.M. Navon, and J.J. O'Brien, Objective analysis of pseudostress over the Indian Ocean using a direct-minimization approach, *Mon. Wea. Rev., 117*, 709-720, 1989.

Liu, W.T., and W. Tang, Spaceborne scatterometer in studies of atmospheric and oceanic phenomena from synoptic to interannual time scales, in *Space Remote Sensing of Subtropical Ocean*, C.T. Liu (ed.), Elsevier Press, New York, 113-125, 1997.

Liu, W.T., W. Tang, and R.S. Dunbar, Scatterometer Observes Extratropical Transition of Pacific Typhoons, *Eos Trans. Amer. Geophys. Union, 78*, 237 & 240, 1997.

Tang, W., and W.T. Liu, Objective Interpolation of Scatterometer Winds, *JPL Publication 96-19*, Jet Propulsion Laboratory, Pasadena, CA.,16 pp, 1996.
Zeng, L., and G. Levy, Space and time aliasing structure in monthly mean polar-orbiting satellite data, *J. Geophys. Res., 100*, 5133-5142, 1995.

Captions

Figure 1. The differences between the weekly averages (13-19 October 1996) of the objectively interpolated and the bin-averaged NSCAT zonal wind component.

Figure 2 The differences between monthly averaged zonal components of NSCAT and ECMWF winds for (from top to bottom) October 1996, December 1996, March 1997, and June 1997, representing the four seasons.

Figure 3 Wind vectors (white arrows) superimposed on wind speed (color image) as derived from NSCAT data (upper) and ECMWF data (center) for December 1996 off the South American coast. The vector and speed differences are also shown. (lower)

Figure 4 Same as Fig. 3, except for eastern equatorial Pacific.

Figure 5 The differences in the two-dimensional wavenumber spectra computed from weekly averaged (13-19 October 1996) NSCAT and ECMWF wind fields in a mid-Pacific area between 32°N and 32°S, 176°E to 304°E.

Figure 1. The differences between the weekly averages (13-19 October 1996) of the objectively interpolated and the bin-averaged NSCAT zonal wind component.

Figure 2 The differences between monthly averaged zonal components of NSCAT and ECMWF winds for (from top to bottom) October 1996, December 1996, March 1997, and June 1997, representing the four seasons. .

Figure 3 Wind vectors (white arrows) superimposed on wind speed (color image) as derived from NSCAT data (upper) and ECMWF data (center) for December 1996 off the South American coast. The vector and speed difference are also shown. (lower)

Figure 4 Same as Fig. 3, except for eastern equatorial Pacific.

Figure 5 The differences in the two-dimensional wavenumber spectra computed from weekly averaged (13-19 October 1996) NSCAT and ECMWF wind fields in a mid-Pacific area between 32°N and 32°S, 176°E to 304°E.

LIU ET AL.: NASA scatterometer provides global ocean-surface wind ..

LIU ET AL.: NASA scatterometer provides global ocean-surface wind ..

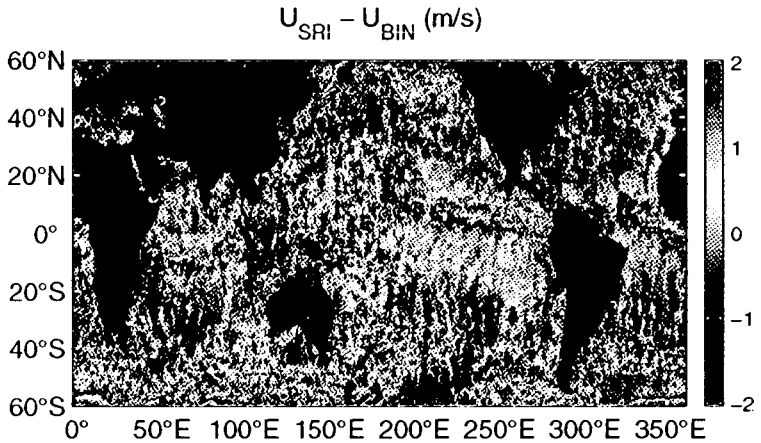
$U_{SRI} - U_{BIN}$ (m/s)
60°N
40°N
20°N
0°
20°S
40°S
60°S
0°
50°E
100°E
150°E
200°E
250°E
300°E
350°E
2
1
0
−1
−2

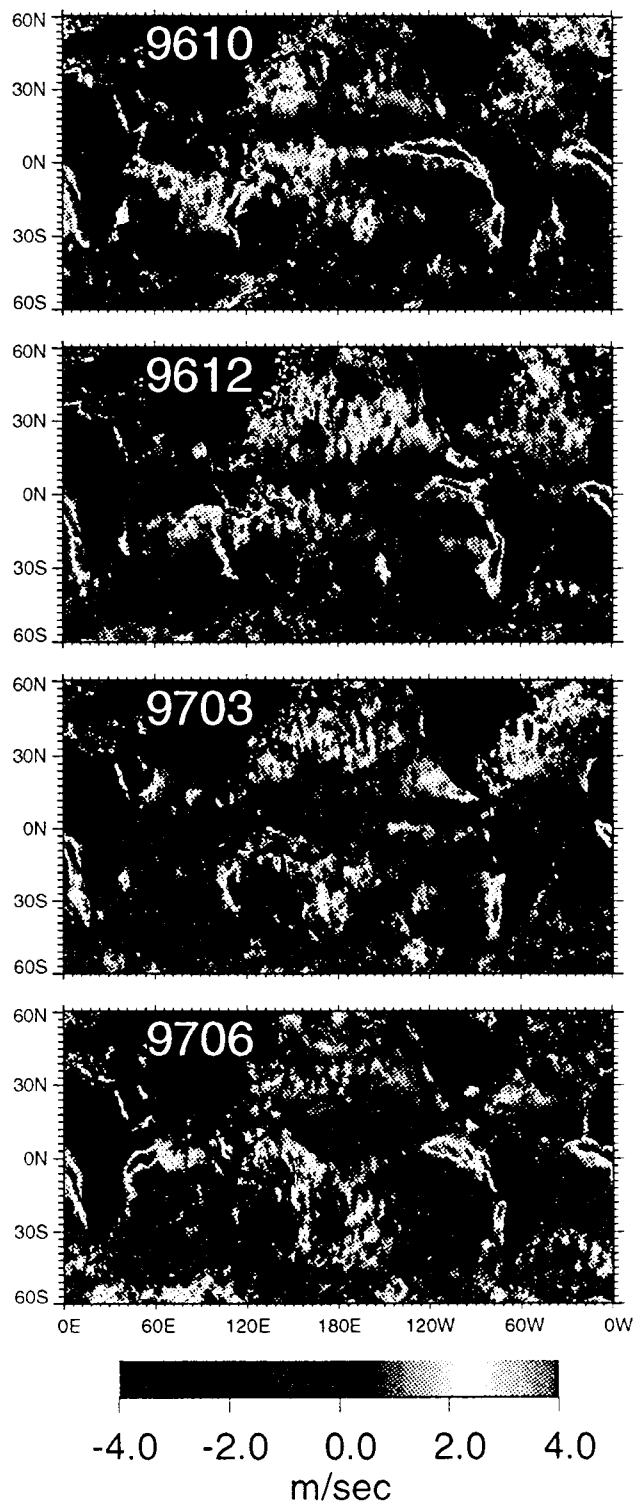
9610
9612
9703
9706
60N
30N
0N
30S
60S
0E
60E
120E
180E
120W
60W
0W
-4.0
-2.0
0.0
2.0
4.0
m/sec

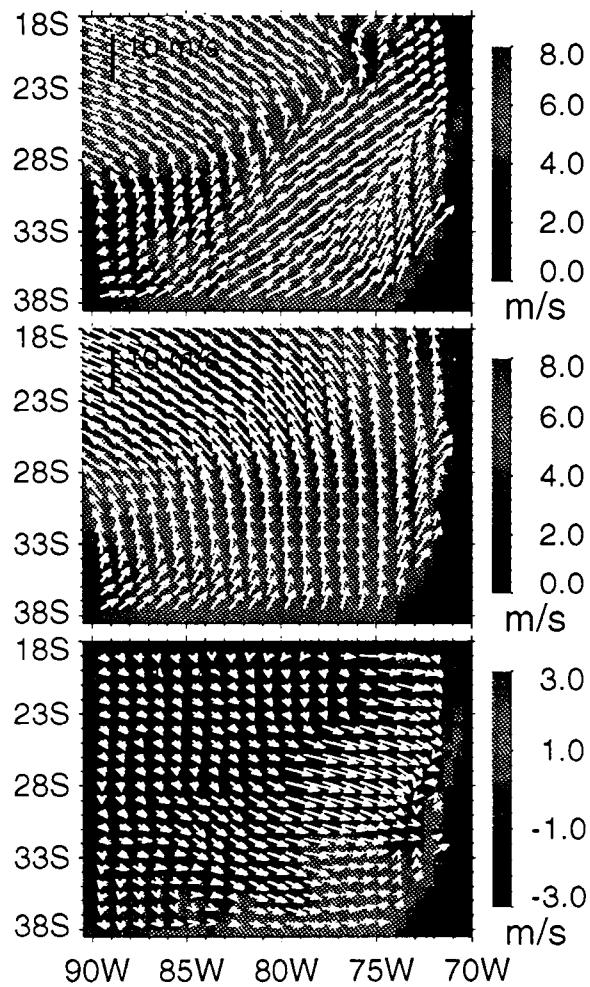
18S
23S
28S
33S
38S
10 m/s
8.0
6.0
4.0
2.0
0.0
m/s
18S
23S
28S
33S
38S
10 m/s
8.0
6.0
4.0
2.0
0.0
m/s
18S
23S
28S
33S
38S
3.0
1.0
-1.0
-3.0
m/s
90W
85W
80W
75W
70W

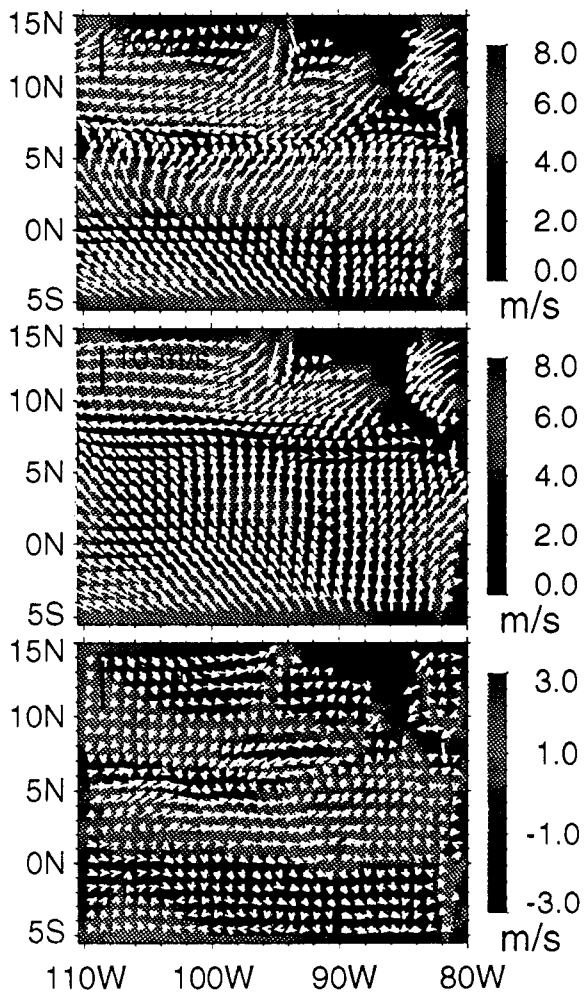
15N
10N
5N
0N
5S
8.0
6.0
4.0
2.0
0.0
m/s
15N
10N
5N
0N
5S
8.0
6.0
4.0
2.0
0.0
m/s
15N
10N
5N
0N
5S
3.0
1.0
-1.0
-3.0
m/s
110W
100W
90W
80W

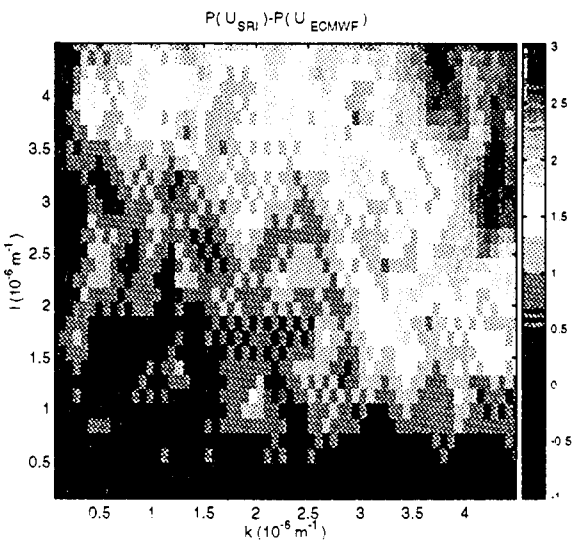
P(U SRI)-P(U ECMWF)
l (10-6 m-1)
k (10-6 m-1)
0.5
1
1.5
2
2.5
3
3.5
4
3
2.5
2
1.5
1
0.5
0
-0.5